arXiv:1702.07897v1 [physics.soc-ph] 25 Feb 2017

# A model bridging chimera state and explosive synchronization

Xiyun Zhang,[1] Hongjie Bi,[1] Shuguang Guan,[1] Jinming Liu,[2] and Zonghua Liu[1,2,*]

[1]*Department of Physics, East China Normal University, Shanghai, 200062, P. R. China*
[2]*State Key Laboratory of Precision Spectroscopy, East China Normal University, Shanghai 200062, China*

(Dated: February 28, 2017)

Global and partial synchronization are the two distinctive forms of synchronization in coupled oscillators and have been well studied in the past decades. Recent attention on synchronization is focused on the chimera state (CS) and explosive synchronization (ES), but little attention has been paid to their relationship. We here study this topic by presenting a model to bridge these two phenomena, which consists of two groups of coupled oscillators and its coupling strength is adaptively controlled by a local order parameter. We find that this model displays either CS or ES in two limits. In between the two limits, this model exhibits both CS and ES, where CS can be observed for a fixed coupling strength and ES appears when the coupling is increased adiabatically. Moreover, we show both theoretically and numerically that there are a variety of CS basin patterns for the case of identical oscillators, depending on the distributions of both the initial order parameters and the initial average phases. This model suggests a way to easily observe CS, in contrast to others models having some (weak or strong) dependence on initial conditions.

PACS numbers: 89.75.-k, 05.45.Xt

## I. INTRODUCTION

Synchronization in coupled oscillators has been well studied in the past decades and is now focused on the influence of network structures [1–3]. In this field, two hot topics are the chimera state (CS) and explosive synchronization (ES), respectively. CS was first found by Kuramoto and Battogtokh in 2002 [4]. After the discovery, CS has attracted a lot of attention in the past decade [6–18]. Generally speaking, CS is the coexistence of coherent and incoherent behaviors in coupled identical oscillators. Because of different initial conditions, the nonlocally coupled oscillators naturally evolve into distinct coherent and incoherent groups. This counterintuitive coexistence of coherent and incoherent oscillations in populations of identical oscillators, each with an equivalent coupling structure, can be considered as a symmetry breaking on the collective behavior by nonsymmetric initial conditions. This phenomenon reminded people the two heads monster in Greek mythology and thus was named as *Chimera State* by Abrams and Strogatz in 2004 [5]. The study of CS was originally motivated by the phenomenon of unihemispheric sleep of many creatures in real world [19–23], which was first found in dolphin and then revealed in birds, some aquatic mammals, and reptiles etc. So far, CS has been confirmed in many experiments [24–30]. For example, Tinsley *et al* reported on experimental studies of CS in populations of coupled chemical oscillators [24]. Hagerstrom *et al* showed experimental observation of CS in coupled-map lattices [25]. Viktorov *et al* demonstrated a coexistence of coherent and incoherent modes in the optical comb generated by a passively mode-locked quantum dot laser [26]. Wickramasinghe *et al* presented the experiment of CS in a network of electrochemical reactions [27]. Martens *et al* devised a simple experiment with mechanical oscillators to show CS [28]. And Schoenleber *et al* reported the CS in the oxide layer during the oscillatory photoelectrodissolution of n-type doped silicon electrodes under limited illumination [30].

ES represents the first-order synchronization transition in networked oscillators. When we increase the coupling strength adiabatically, the system stays unsynchronized until a critical forward coupling strength $\lambda_{cF}$ where the system suddenly becomes synchronized. That is, its order parameter $R$ has a jump at $\lambda_{cF}$. However, when we decrease the coupling strength adiabatically from a synchronized state, the system does not go back by the same route as the forward process but jump at a different critical backward coupling strength $\lambda_{cB}$. As $\lambda_{cF} > \lambda_{cB}$, the forward and backward routes of $R$ forms a hysteresis loop. This first-order transition was in fact found before the concept of complex networks [31–33] and became hot only when it was rediscovered from the positive correlation between the natural frequency of a networked oscillator and its degree by Gómez-Gardeñes *et al* and named as *Explosive Synchronization* in 2011 [34]. Before the work [34], synchronization on complex networks was generally analyzed by the approach of master stability function [35], which always predicts a second-order phase transition. However, the work [34] showed that it is also possible for the synchronization on complex networks to be the first-order, thus inducing great attention on ES [36–48]. It was revealed that except the way in [34], ES can be also observed by many other ways, providing that the growth of synchronized clusters is under a suppressive rule [49].

Currently, CS and ES are separately studied as two distinctive topics. In general, we do not have CS in the systems of ES, and vice versa. Thus, it is interesting to ask whether it is possible to observe both of them in a single system. To figure out the answer, we here study this topic by presenting a novel model to bridge these two phenomena. The model consists of two groups of coupled nonidentical oscillators with a natural frequency distribution. Specifically, its coupling strength is adaptively controlled by a parameter $\beta$. This model goes back to the standard CS model [21] when all the natural frequencies

*Electronic address: zhliu@phy.ecnu.edu.cn

are the same and $\beta = 0$ and returns to the adaptive model of ES [48] when there is only one group of oscillators and $\beta = 1$. Very interesting, we find that this model displays both CS and ES, where CS can be observed for a fixed coupling strength and ES appears when the coupling is increased adiabatically. Thus, this model sets up a bridge between CS and ES. Moreover, we focus on the case of identical oscillators and show both theoretically and numerically that there are a variety of CS basin patterns, depending on the distributions of both the initial order parameters and the initial average phases. That is, this model shows a way to easily observe CS, in contrast to the sensitive dependence on initial conditions in many previous models [50, 51].

The paper is organized as follows. In Sec.II, we introduce the model and study its collective behaviors. In Sec.III, we pay attention to the case of identical oscillators and study it by the dimensional reduction analysis. In Sec. IV, we show the corresponding numerical simulations and and its stability analysis. Finally, in Sec. V, we give conclusions and discussions.

## II. MODEL DESCRIPTION

We consider a model of two groups of coupled oscillators, defined as

$$\begin{aligned}\dot{\theta}_{i,j} &= \omega_{i,j} + \frac{R_j^\beta \lambda}{N}\sum_{k=1}^{N}\sin(\theta_{k,j} - \theta_{i,j} + \alpha) \\ &+ \frac{R_j^\beta \lambda'}{N}\sum_{k=1}^{N}\sin(\theta_{k,j'} - \theta_{i,j} + \alpha), \end{aligned} \quad (1)$$

where the index $j = 1, 2$ represents the two groups, $i = 1, \cdots, N$ represents the $N$ oscillators in each group. $\omega_{i,j}$ is the natural frequency satisfying an uniform distribution in $(-\delta, \delta)$. The oscillators are globally coupled with coupling strength $\lambda$ inside each group and coupling strength $\lambda'$ between the two groups. $j'$ represents the other group, defined as $j' = 2$ when $j = 1$ and $j' = 1$ when $j = 2$. $\alpha$ is a phase lag parameter and set as $\alpha = \frac{\pi}{2} - 0.1$, which was chosen by many CS papers [21–23]. The coupling is attractive when $\alpha < \pi/2$ and repulsive when $\alpha > \pi/2$. $\beta$ is a parameter located in $[0, 1]$.

$R_1$ and $R_2$ in Eq. (1) are the order parameters of the groups 1 and 2, respectively, which are defined as

$$R_1 e^{i\Psi_1} = \frac{1}{N}\sum_{k=1}^{N} e^{i\theta_{k,1}}, \quad R_2 e^{i\Psi_2} = \frac{1}{N}\sum_{k=1}^{N} e^{i\theta_{k,2}}. \quad (2)$$

In the framework of Eq. (1), the population is put into two groups and the coupling strengthes $R_j^\beta \lambda$ and $R_j^\beta \lambda'$ are closely correlated to the local coherence when $\beta$ is not 0. The model (1) will return to the case of one population in Ref. [48] when $\lambda' = 0$ and $\beta = 1$. To show the influence of $\beta$, Fig. 1 shows the synchronization transition of model (1) for different $\beta$, with $\lambda' = 0$. It's easy to see that $R$ has a continuous transition for $\beta = 0$, a discontinuous transition for $\beta = 1$, and a transition gradually changing from continuous to discontinuous when $\beta$ increases, indicating a transition from traditional synchronization to explosive synchronization. When $\beta$ is in the range of hysteresis loop, there are bistability where the final state of system depends sensitively on the initial conditions.

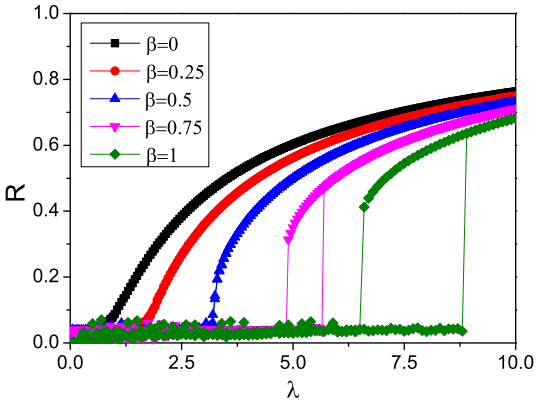


FIG. 1: (color online). Synchronization transition of model (1) with only one population, i.e. $\lambda' = 0$. The parameters are $\delta = 1.0$ and $\alpha = \frac{\pi}{2} - 0.1$

The model (1) is more sensitive to the local coherence if there are two or more groups in the system. Once the initial conditions are asymmetric, the two groups may easily go to different final states, i.e. one group with high coherence and another group with low coherence.

Eq. (1) has two limiting behaviors. The first one is the limiting behavior of $\lambda' = 0$ and $\beta = 1$, which goes back to the adaptive model of ES in Ref. [48]. In this situation, ES can be observed if we increase (decrease) the coupling adiabatically in the forward (backward) continuation diagram. Fig. 2(a) shows the dependence of $R_1$ on $\lambda$ for $\delta = 1.0$. It is easy to see that there is a hysteresis loop, indicating the existence of ES. The inset of Fig. 2(a) shows the evolution of two different initial conditions for $\lambda = 8.5$. We see that one gradually approaches a higher value ($R_1 \approx 0.58$) and the other goes to zero, confirming the sensitivity to initial conditions in the bistable region. We have the same results for $R_2$ of another group (it's not shown in Fig. 2 ), as the system exhibits the symmetry $1 \leftrightarrow 2$.

The second one is the limiting behavior of identical $\omega_{i,j}$ ($\delta = 0$) in Eq. (1) for all the oscillators and $\beta = 0$, which returns to the typical model of CS in Ref. [21]. In this case, our numerical simulations confirm that one group is synchronized with $R_1 = 1$ while the other is unsynchronized with $R_2 < 1$. Furthermore, we were surprised to find that there is still a chimera-like behavior when we keep $\beta = 0$ but let $\omega_{i,j}$ satisfy the uniform distribution in $(-\delta, \delta)$. Figure 3 (a)-(d) show the results for $\delta = 1.0, 0.5, 0.2$ and $0.15$, respectively. We see that the oscillation periods of $R_1$ and $R_2$ increase with the decrease of $\delta$ until $\delta = 0.15$. After that, the oscillation behaviors of $R_1$ and $R_2$ will disappear and are replaced by

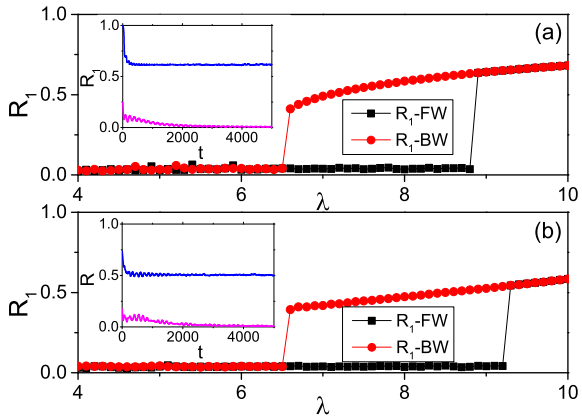


FIG. 2: (color online). (a) Case of $\lambda' = 0$ with $\delta = 1.0$, $\alpha = \frac{\pi}{2} - 0.1$ and $\beta = 1$. The "squares" and "circles" represent $R_1$ for the forward and backward continuation diagram, respectively. The inset shows the evolution of two different initial conditions for $\lambda = 8.5$. (b) Case of $\lambda' = 2$ with $\delta = 1.0$, $\alpha = \frac{\pi}{2} - 0.1$ and $\beta = 1$. The "squares" and "circles" represent $R_1$ for the forward and backward continuation diagram ($R_2$ has the same loop but not shown here), respectively. The two curves in the inset show the evolution of two typical $R_1$ and $R_2$ in the two groups, respectively, with $\lambda = 8.5$.

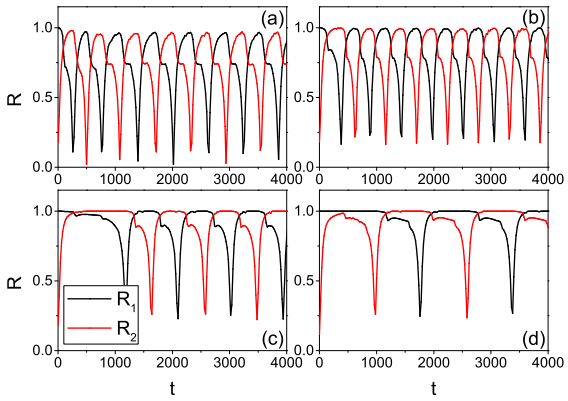


FIG. 3: (color online). The chimera-like behaviors in Eq. (1) for $\beta = 0, \lambda = 8.0$ and $\lambda' = 3.0$ where the black and red line represent $R_1$ and $R_2$, respectively, and (a)-(d) represent the cases of $\delta = 1.0, 0.5, 0.2$ and $0.15$, respectively.

one group synchronized and the other unsynchronized, i.e. chimera state.

We now go back to the current model of Eq. (1) with $\beta = 1$. We find that it can also show the hysteresis loop. Fig. 2(b) shows the results of $R_1$ for $\lambda' = 2$. Comparing Fig. 2(b) with Fig. 2(a) we see that their forward jumping positions are slightly different, i.e. $\lambda_{cF} < 9.0$ in Fig. 2(a) while $\lambda_{cF} > 9.0$ in Fig. 2(b). We have observed the same results for $R_2$ (not shown here), as the symmetry $1 \leftrightarrow 2$ in the two groups of the system. The inset of Fig. 2(b) shows the evolution of two typical initial conditions from the two groups, respectively,

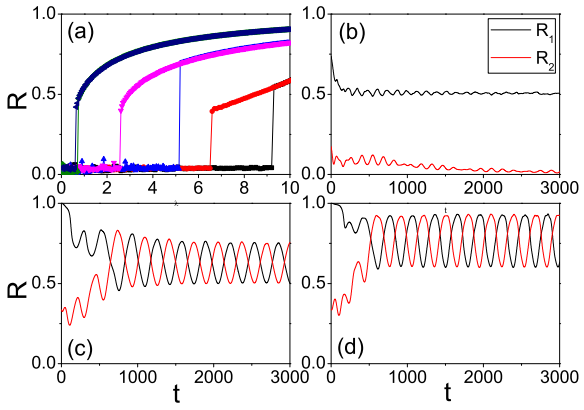


FIG. 4: (color online). Coexistence of ES and CS in the model of Eq. (1) for $\alpha = \frac{\pi}{2} - 0.1$, $\beta = 1$, and $\lambda' = 2$. (a) $R_1$ versus $\lambda$ where the "black" and "red" lines represent $R_1$ of the forward and backward continuation diagram for $\delta = 1$, respectively; the "blue" and "pink" lines represent the case of $\delta = 0.7$; and the "dark green" and "dark blue" lines represent the case of $\delta = 0.4$. (b)-(d) Evolutions of $R_1$ and $R_2$ on time $t$ for $\lambda = 8.0$ and $\delta = 1, 0.7$ and $0.4$, respectively.

for $\lambda = 8.5$. We see that one ($R_1$) goes to a higher value ($R_1 \approx 0.58$) and the other ($R_2$) goes to zero, indicating a chimera-like behavior. Therefore, we have observed both ES and CS in the model of Eq. (1) when the parameters are taken in the range of the hysteresis loop.

Then, we change the range of frequency distribution $\delta$. We find that the hysteresis loop depends on the parameter $\delta$ and can be observed only when $\delta > 0.31$. With the decrease of $\delta$, the size of the loop decreases until zero at about $\delta = 0.31$ and the transition points of $R_1$ or $R_2$ also approaches zero. Fig. 4(a) shows the results for $\lambda' = 2$, where the "squares" and "circles" represent $R_1$ of the forward and backward continuation diagram for $\delta = 1$, respectively; the "up triangles" and "down triangles" represent the case of $\delta = 0.7$; and the "diamonds" and "left triangles" represent the case of $\delta = 0.4$. To check the coexistence of CS, we study the evolution of $R_1$ and $R_2$ for two different initial conditions. Fig. 4(b)-(d) show the results for $\lambda = 8.0$ and $\delta = 1, 0.7$ and $0.4$, respectively. We see that Fig. 4(b) is a chimera-like state while Fig. 4(c) and (d) are breather-like states. In sum, the range of frequency distribution $\delta$ takes a key role for the coexistence of ES and CS.

## III. DIMENSIONAL REDUCTION ANALYSIS

In the following parts, we study CS in model (1) with $\beta = 1$. In order to satisfy the definition of CS, we change to identical oscillators ($\delta = 0$). To make a theoretical analysis on Eq. (1), it is better to reduce its dimension. Fortunately, such an approach of dimensional reduction has been proposed by Watanabe and Strogatz [52] and then generalized by Pikovsky and Rosenblum [53]. We here adopted it to analyze the model (1). In a mean-field framework, the coupling terms in Eq. (1)

can be rewritten as $R_a^2\lambda\sin(\Psi_a-\theta_j^a+\alpha)+R_aR_{a'}\lambda'\sin(\Psi_{a'}-\theta_j^a+\alpha)$. Thus, Eq. (1) can be rewritten as

$$\begin{aligned}\dot{\theta}_j^a &= Im(Z_a e^{-i\theta_j^a})\\ Z_a &= R_a^2\lambda e^{-i(\Psi_a+\alpha)}+R_aR_{a'}\lambda' e^{-i(\Psi_{a'}+\alpha)},\end{aligned} \quad (3)$$

where $Z$ is the mean field coupling for the oscillator $j$, $a$ and $a'$ are the index of the two populations, respectively. The average frequency $\langle\omega\rangle$ has been ignored as it is zero for a symmetric distribution. By introducing three variables $\rho_a(t)$, $\Theta_a(t)$, $\Phi_a(t)$ and constants $\psi_j^a$ via the transformation

$$\tan[\frac{\theta_j^a-\Phi_a}{2}]=\frac{1-\rho_a}{1+\rho_a}\tan[\frac{\psi_j^a-\Theta_a}{2}], \quad (4)$$

we get the WS equations of the Eq. (1) [52, 53]

$$\begin{aligned}\dot{\rho}_a &= \frac{1-\rho_a^2}{2}Re(Z_a e^{-i\Phi_a})\\ \dot{\Theta}_a &= \frac{1-\rho_a^2}{2\rho_a}Im(Z_a e^{-i\Phi_a})\\ \dot{\Phi}_a &= \frac{1+\rho_a^2}{2\rho_a}Im(Z_a e^{-i\Phi_a}).\end{aligned} \quad (5)$$

Generally, the parameter $\rho$ characterizes the degree of synchronization: $\rho=0$, if the oscillators are incoherent, and $\rho=1$, if the oscillators are complete synchronized. $\rho_a$ is roughly proportional to the order parameter $R_a$. The phase variable $\Theta$ describes the shift of individual oscillators with the mean phase and $\Phi$ describes the average of the phases. It is convenient to introduce new variables $\xi_a=\Phi_a-\Theta_a$ and $z_a=\rho_a e^{i\Phi_a}$, then Eq. (5) can be rewritten as

$$\dot{z}_a = \frac{1}{2}Z_a-\frac{z_a^2}{2}Z_a^* \quad (6)$$

$$\dot{\xi}_a = Im(z_a^*Z_a). \quad (7)$$

If the constants $\psi_j^a$ are uniformly distributed, Eqs. (6) and (7) will decouple. Eq. (6) describes the low dimensional behavior of Eq. (1). In the thermodynamic limit, we have $\rho_a=R_a$ and thus from Eq. (6) we obtain

$$\begin{aligned}\dot{R}_a &= \frac{1}{2}R_a(1-R_a^2)[\lambda R_a\cos\alpha+\lambda' R_{a'}\cos(\Phi_{a'}-\Phi_a+\alpha)]\\ \dot{\Phi}_a &= \frac{1}{2}(1+R_a^2)[\lambda R_a\sin\alpha+\lambda' R_{a'}\sin(\Phi_{a'}-\Phi_a+\alpha)].\end{aligned} \quad (8)$$

Eq. (8) describes the theoretical prediction of the collective behaviors of Eq. (1). However, it is not easy to get the precise solution of Eq. (8). Hence, we here calculate Eq. (1) numerically. In this way, the initial order parameters $R_1(0)$ and $R_2(0)$ and the initial phases $\Phi_1(0)$ and $\Phi_2(0)$ will be the key factors to influence the final states $R_1$ and $R_2$.

## IV. RESULTS AND ANALYSIS

In numerical simulations, we take the system size as $2N=100$, i.e. $N=50$ for each group. For the convenience of comparing with the above theoretical predictions, we let all the natural frequencies $\omega_{i,j}$ in Eq. (1) be zero. The initial phases are drawn from the circular Cauchy distribution [54]

$$g(\theta(0))=\frac{1-|\gamma|^2}{2\pi|e^{i\theta}-\gamma|^2} \quad (9)$$

which can be easily generated from a Lorentzian distribution $g(x)=\frac{1}{\pi}[\frac{\eta}{(x-x_0)^2+\eta^2}]$ with $\eta$ being the half width at half maximum and $x_0$ being the center frequency. Making a transformation $X=\frac{x+i}{x-i}$, we can get a new complex variable $X$, which is distributed on a unit circular in complex plane. The phases of $X$ are distributed as circular Cauchy distribution. By changing $x_0$ and $\eta$, we can easily change the average and deviation of the circular Cauchy distribution and thus change the initial order parameter of the oscillators. In this way, we have observed a variety of CS patterns in the two groups. Figs. 5(a) and (b) show two typical CS patterns after the transient process, where (a) denotes the case of coupling strength $\lambda=\lambda'=1$ and the initial order parameter $R_1(0)=0.275$ and $R_2(0)=0.569$, and (b) denotes the case of coupling strength $\lambda=1.5$ and $\lambda'=1$ and the initial order parameters $R_1(0)=0.1$ and $R_2(0)=0.569$. We see that in each case, one group is synchronized with $R_2=1$ and the other has a different $R_1<1$, implying a breathing CS. In contrast, we numerically calculate the theoretical Eq. (8) and show the results in Figs. 5 (c) and (d), where the difference between the initial phases of the two groups is taken as $\Delta\Phi=\Phi_2(0)-\Phi_1(0)=2\pi/3$. In fact, Figs. 5 (c) and (d) can be considered as the corresponding theoretical results of Figs. 5(a) and (b). Comparing Fig. 5 (a) with (c) and Fig. 5(b) with (d), respectively, we see that the theoretical results are qualitatively consistent with the numerical simulations.

To show the dependence of CS on the initial conditions in details, we first fix the initial average phases as $\Delta\Phi=\Phi_2(0)-\Phi_1(0)=2\pi/3$ and let the initial order parameters $R_1(0)$ and $R_2(0)$ gradually increase from 0 to 1 by changing $x_0$ and $\eta$. Figs. 6(a) and (b) show how the stabilized $R_1$ and $R_2$ depend on the initial $R_1(0)$ and $R_2(0)$. Comparing Fig. 6(a) with (b) we see that $R_1$ is low when $R_2$ is high, and vice versa, i.e. they are complementary, indicating that the whole system is always in CS. This is an interestingly finding which tells us that no matter what the initial conditions are, we can always find one group in high coherence while the other in low coherence, indicating that the basin of CS in the model of Eq. (1) is the whole initial condition space or CS is robust to initial conditions. This feature is very different from some of the previous models of CS, where CS is typically observed for carefully chosen initial conditions. We also show the corresponding theoretical results from Eq. (8) in Figs. 6(c) and (d). Comparing Fig. 6(a) with (c) and Fig. 6(b) with (d), respectively, we see that they are almost the same, indicating the consistence between the numerical simulations and theoretical results.

Then, we study the influence of the initial average phases. For this purpose, we consider a variety of difference $\Delta\Phi=\Phi_2(0)-\Phi_1(0)$. As $\Delta\Phi$ is not neglected in Eq. (8) of the dimensional reduction, the low dimensional analysis shows the same effect with the numerical simulations by the circular

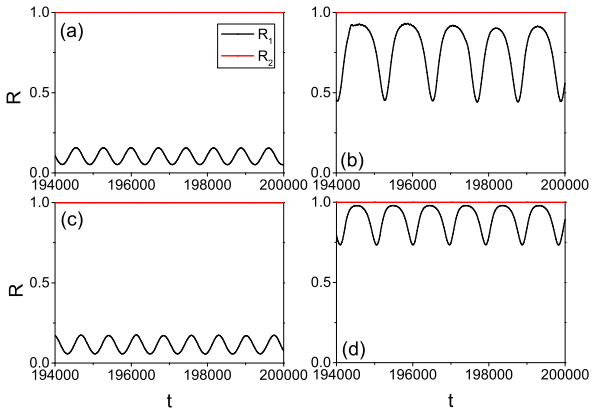


FIG. 5: (color online). Comparison between numerical simulations and theoretical results where (a) and (b) represent the numerical simulations from Eq. (1) with $\omega_{i,j} = 0$ and (c) and (d) the corresponding theoretical results from Eq. (8). (a) and (c): The coupling strength is $\lambda = \lambda' = 1$ and the initial order parameters are taken as $R_1(0) = 0.275$ and $R_2(0) = 0.569$. The difference between the initial average phase is $\Delta\Phi = \Phi_2(0) - \Phi_1(0) = 2\pi/3$. (b) and (d): The coupling strengthes are $\lambda = 1.5$ and $\lambda' = 1$ and the initial order parameters are taken as $R_1(0) = 0.1$ and $R_2(0) = 0.569$. The difference between the initial average phases is also taken as $\Delta\Phi = \Phi_2(0) - \Phi_1(0) = 2\pi/3$.

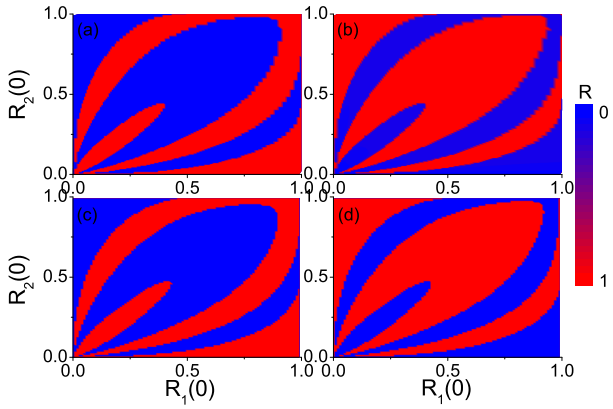


FIG. 6: (color online). Influence of the initial order parameters $R_1(0)$ and $R_2(0)$ on the stabilized $R_1$ and $R_2$ in the two groups. (a) and (b) show the results of numerical simulations for $R_1$ and $R_2$ from Eq. (1), respectively. (c) and (d) show the theoretical results from Eq. (8), corresponding to (a) and (b), respectively. The difference between the initial average phases are all $\Delta\Phi = 2\pi/3$ and the coupling strength is $\lambda = \lambda' = 1$.

Cauchy distributed initial conditions. For this reason, we here only calculate the theoretical solution of Eq. (8). We find that the stabilized CS do depend on the specific value of the initial average phases. As $R_1$ and $R_2$ are complementary, we here only calculate the stabilized $R_1$. Figure 7 shows four typical cases where (a)-(d) represent the cases of $\Delta\Phi = \pi/3, \pi, \pi/2$

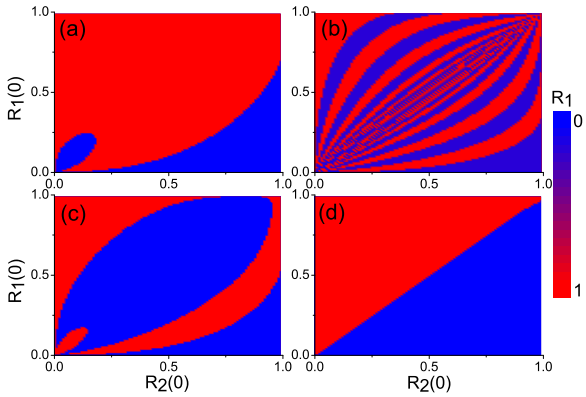


FIG. 7: (color online). Influence of different initial average phases $\Delta\Phi = \Phi_2(0) - \Phi_1(0)$ on the patterns of CS where the parameters are the same as in Fig. 6. The results are obtained for the stationary $R_1$ by the theoretical analysis Eq. (8). (a) Case of $\Delta\Phi = \pi/3$; (b) Case of $\Delta\Phi = \pi$; (c) Case of $\Delta\Phi = \pi/2$; and (d) Case of $\Delta\Phi = 0$.

and 0, respectively. It is easy to see that the four patterns in Fig. 7 are different, indicating the diversity of the CS basin patterns for different initial conditions.

The robustness of CS to initial conditions is very interesting. To understand it better, we follow the Ref. [21] to make a further analysis on Eq. (8). Firstly, we introduce a new parameter $A = \lambda - \lambda'$. As all the frequencies of oscillators are zero, we rescale the coupling as $1 = \lambda + \lambda'$ and thus obtain $\lambda = (1 + A)/2$ and $\lambda' = (1 - A)/2$. Therefore, $A = 0$ represents the case of $\lambda = \lambda'$, while $A = 1$ represents the case of $\lambda' = 0$, i.e. only one group of population. Then, we introduce $\Delta\Phi = \Phi_2 - \Phi_1$. For a typical CS, one population is synchronized with $R = 1$, thus we can set its order parameter as unity, i.e. $R_1 = 1$ and $\dot{R}_1 = 0$. By this way, the Eq. (8) becomes

$$\begin{aligned}
\dot{R}_2 &= \frac{1}{2}R_2(1-R_2^2)[\frac{1+A}{2}R_2\cos\alpha \\
&\quad + \frac{1-A}{2}\cos(-\Delta\Phi+\alpha)] \\
\Delta\dot{\Phi} &= \frac{1}{2}(1+R_2^2)[\frac{1+A}{2}R_2\sin\alpha + \frac{1-A}{2}\sin(-\Delta\Phi+\alpha)] \\
&\quad -[\frac{1+A}{2}\sin\alpha + \frac{1-A}{2}R_2\sin(\Delta\Phi+\alpha)]. \qquad (10)
\end{aligned}$$

By letting $\dot{R}_2 = 0$, we can get three solutions: $R_2 = 1$, $R_2 = 0$ and $R_2 = -\frac{(1-A)\cos(\alpha-\Delta\Phi)}{(1+A)\cos\alpha}$. The first solution means a complete synchronized state and the other two mean CS. By checking the values of $R_1$ and $R_2$ in both Fig. 6 and Fig. 7, we find that all the blue areas are in between 0.1 and 0.2, indicating that they are the third solution. Therefore, we here focus only on the first two solutions, i.e. $R_2 = 1$ and $R_2 = 0$. The Jacobian matrix of Eq. (10) is

$$M = \begin{bmatrix} a & b \\ c & d \end{bmatrix} \qquad (11)$$

with

$$
\begin{aligned}
a &= \frac{1+A}{2}R_2\cos\alpha + \frac{1-A}{4}\cos(\alpha-\Delta\Phi) \\
&\quad -(1+A)R_2^3\cos\alpha - \frac{3(1-A)}{4}R_2^2\cos(\alpha-\Delta\Phi) \\
b &= \frac{1}{2}R_2(1-R_2^2)\sin(\alpha-\Delta\Phi) \\
c &= \frac{1+A}{4}\sin\alpha + \frac{3(1+A)}{4}R_2^2\sin\alpha \\
&\quad +\frac{1-A}{2}R_2\sin(\alpha-\Delta\Phi) - \frac{1-A}{2}\sin(\Delta\Phi+\alpha) \\
d &= -\frac{1-A}{4}(1+R_2^2)\cos(\alpha-\Delta\Phi) \\
&\quad -\frac{1-A}{2}R_2\cos(\Delta\Phi+\alpha). \qquad (12)
\end{aligned}
$$

By using of the linear stability analysis we find that the solution of $R_2 = 0$ is unstable while $R_2 = 1$ is stable with the same parameters of Figs. 6 and 7. It means that there is a probability to observe the complete synchronization in the initial condition space. With further linear stability analysis, we find that the invariant manifold with $R_1 = R_2$ found in [50] still exists. In order to check this point, we fix the average of initial order $\langle R(0)\rangle = (R_1(0) + R_2(0))/2$ and look for the basin of the states in the plane of $\Delta R(0) = R_1(0) - R_2(0)$ and $\Delta\Phi(0)$, i.e. taking the same way as Ref. [50] did. Fig. 8(a) shows the distribution of the stabilized state for the case of $\langle R(0)\rangle = 0.75$, where DS means the first group is synchronized while the second one is desynchronized, SD means the second group is synchronized while the first one is desynchronized, and SS means both of the two groups are synchronized. Thus, DS and SD are CS while SS is a complete synchronized state. From this figure, we see the basin of complete synchronized state (SS) is very narrow and it occurs only when the system changes from DC state to SD state or the vice versa, which is the same as in Ref. [50]. To see it more clear, Fig. 8(b) shows the basin of synchronized state only, where the basin of CS is hidden. These basins of complete synchronized state are too narrow and thus make the SS state not easy to be observed, which is the reason why we miss the complete synchronized state in Figs. 6 and 7. On the other hand, we notice that in Fig. 8, the basins of the states are spiral shaped around the point $\Delta R(0) = 0$, $\Delta\Phi(0) = \pi$, indicating the influence of the initial phases. This is very similar with the result of Ref. [50].

In order to show how the basins of CS change with parameters, we calculate the probability of chimera state with different initial conditions in the parameter plane of $A$ versus $\pi/2 - \alpha$. Fig.9 shows the results. It is easy to see that the probability of CS decreases with the decreasing of $\alpha$. When $A$ is large, the probability of of CS becomes zero.

## V. DISCUSSION

To connect CS and ES, Eq. (1) has three key aspects. The first one is the asymmetric couplings $\lambda$ and $\lambda'$. When $\lambda > \lambda'$, the coupling in each group is greater than that between the two groups. Thus, the oscillators may be synchronized in their own groups but remain unsynchronized to those in another group. The second one is the control parameter $\beta$. It guarantees the appearance of ES. And the third one is the range parameter of the natural frequencies $\delta$. When $\delta$ is relatively large, we have both ES and CS-like behaviors. When $\delta$ is relatively small, we only have CS. In this sense, we may also consider $\delta$ as the parameter connecting CS and ES.

One advantage of Eq. (1) is that its CS can be easily ob-

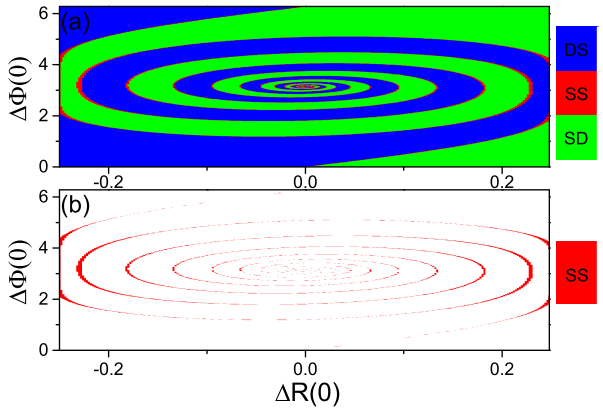


FIG. 8: (color online). Influence of the initial order parameters, $\Delta R(0)$ and $\Delta\Phi(0)$, on the stabilized $R_1$ and $R_2$ in the two groups with the same parameters as Fig. 6 and 7, i.e. $A = 0$. The average of initial order parameter is $\langle R(0)\rangle = (R_1(0) + R_2(0))/2 = 0.75$. Results are obtained by solving the Eq. (10). (a) shows the distribution of the stabilized state where DS means the first group is synchronized while the second group is desynchronized; SD means the second group is synchronized while the first group is desynchronized; and SS means both of the two groups are synchronized. (b) shows the basin of complete synchronized state only, where the basin of CS is hidden.

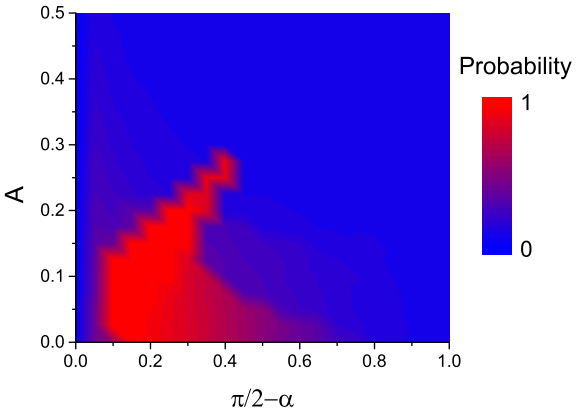


FIG. 9: (color online). Probability of CS when using different initial conditions in the case of different $A$ and $\alpha$, where the results are obtained by solving the Eq. (10).

served. The underlying mechanism may be the bistability. It is known that CS is a kind of symmetry breaking of coherence, due to the symmetry breaking in initial conditions. If a system shows CS, its oscillators should have multi or bistability so that the sensitivity to initial conditions can evolve into the final coexisting behaviors of coherence and incoherence in different population groups. Thus, the multi or bistability is the necessary condition for CS. On the other hand, a characteristic feature of ES is the existence of a hysteresis loop in the order parameter. When coupling strength is located in this hysteresis region, the system has two stable states with one high coherence and the other low coherence, separated by an unstable state. When the coupling is increased adiabatically in the bistable region, the feature of low (high) coherence is remained and thus result in the hysteresis loop, indicating that the bistability is also the necessary condition for ES. Therefore, the bistability is the common basis of CS and ES.

Because of the correlation between local order parameter and coupling strength, our model is more sensitive to symmetry breaking of initial conditions, which makes CS be observed easier. On the other hand, we find that in our model, the basin of CS can be very large, which is similar with the large basin of CS in Refs. [50, 51]. The spiral-shaped basin of states is also similar with the basin structure in [50], and reminds us the spiral wave chimeras in [10] although they are different phenomena.

In conclusion, we have presented a model to describe both CS and ES. We reveal that in two limits, the system goes to CS or ES, respectively. While in between the two limits, the model can show both CS and ES at the same coupling strength. The frequency distribution parameter $\delta$ may seriously influence the final state. When all the natural frequencies are zero, CS is robust to initial conditions and thus, a diversity of the CS basin patterns can be observed. These findings have been confirmed by both numerical simulations and theoretical analysis, which improves our understanding on both CS and ES, especially on their connection.

X.Z. thanks Prof. Arkady Pikvosky for many useful discussions. The authors thank the reviewers for their valuable comments. This work was partially supported by the NNSF of China under Grant Nos. 11135001 and 11375066, 973 Program under Grant No. 2013CB834100, and the Open Fund from the SKLPS of ECNU.

[1] A. Pikvosky, M. Rosenblum, and J. Kurths, *Synchronization: A Universal Concept in Nonlinear Sciences* (Cambridge University Press, Cambridge, 2003).
[2] S. Boccaletti, V. Latora, and Y. Moreno, Phys. Rep. **424**, 175C308 (2006).
[3] A. Arenas, A. Diaz-Guilera, J. Kurths, Y. Moreno, and C. Zhou, Phys. Rep. **469**, 93 (2008).
[4] Y. Kuramoto and D. Battogtokh, Nonlin. Phenom. Complex Syst. **5**, 380 (2002).
[5] D. M. Abrams and S. H. Strogatz, Phys. Rev. Lett. **93**, 174102 (2004).
[6] O. E. Omelchenko, Y. L. Maistrenko, and P. A. Tass, Phys. Rev. Lett. **100**, 044105 (2008).
[7] G. C. Sethia, A. Sen, and F. M. Atay, Phys. Rev. Lett. **100**, 144102 (2008).
[8] G. Bordyugov, A. Pikovsky, and M. Rosenblum, Phys. Rev. E **82**, 035205 (2010).
[9] C. R. Laing, Physica (Amsterdam) D **238**, 1569 (2009); Chaos **19**, 013113(2009).
[10] E. A. Martens, C. R. Laing, and S. H. Strogatz, Phys. Rev. Lett. **104**, 044101 (2010).
[11] M. Wolfrum, O. E. Omelchenko, S. Yanchuk, and Y. L. Maistrenko, Chaos **21**, 013112 (2011).
[12] C. R. Laing, K. Rajendran, and I. G. Kevrekidis, Chaos **22**, 013132 (2012).
[13] Y. Zhu, Y. Li, M. Zhang, and J. Yang, Europhys. Lett. **97**, 10009 (2012).
[14] M. J. Panaggio and D. M. Abrams, Phys. Rev. Lett. **110**, 094102 (2013).
[15] D. Dudkowski, Y. Maistrenko, and T. Kapitaniak, Phys. Rev. E **90**, 032920 (2014).
[16] I. Omelchenko, A. Provata, J. Hizanidis, E. Schöll, and P. Hövel, Phys. Rev. E **91**, 022917 (2015).
[17] P. Jaros, Y. Maistrenko, and T. Kapitaniak, Phys. Rev. E **91**, 022907 (2015).
[18] F. Böhm, A. Zakharova, E. Schöll, and K. Lüdge, Phys. Rev. E **91**, 040901 (2015).
[19] N. C. Rattenborg, C. J. Amlaner, and S. L. Lima, Neurosci. Biobehav. Rev. **24**, 817 (2000).
[20] C. G. Mathews, J. A. Lesku, S. L. Lima, and C. J. Amlaner, Ethology **112**, 286 (2006).
[21] D. M. Abrams, R. Mirollo, S. H. Strogatz, and D. A. Wiley, Phys. Rev. Lett. **101**, 084103 (2008).
[22] A. Pikovsky and M. Rosenblum, Phys. Rev. Lett. **101**, 264103 (2008).
[23] R. Ma, J. Wang, and Z. Liu, Europhys. Lett.**91**, 40006 (2010).
[24] M. R. Tinsley, S. Nkomo, and K. Showalter, Nat. Phys. **8**, 662 (2012).
[25] A. M. Hagerstrom et al., Nat. Phys. **8**, 658 (2012).
[26] E. A. Viktorov, T. Habruseva, S. P. Hegarty, et al., Phys. Rev. Lett. **112**, 224101 (2014).
[27] M. Wickramasinghe and I. Z. Kiss, Phys. Chem. Chem. Phys.**16**, 18360 (2014).
[28] E. A. Martens, S. Thutupalli, A. Fourrire, and O. Hallatschek, Proc. Natl. Acad. Sci. **110**, 10563(2013).
[29] L. Larger, B. Penkovsky, and Y. Maistrenko, Phys. Rev. Lett. **111**, 1(2013).
[30] K. Schoenleber, C. Zensen, A. Heinrich, and K. Krischer, New J. Phys. **16**, 63024 (2014).
[31] S. H. Strogatz, C. M. Marcus, R. M. Westervelt, and R. E. Mirollo, Physica D **36**, 23 (1989).
[32] H.-A. Tanaka, A. J. Lichtenberg, and S. Oishi, Physica D **100**, 279 (1997).
[33] D. Pazó, Phys. Rev. E **72**, 046211 (2005).
[34] J. Gómez-Gardeñes, S. Gómez, A. Arenas, and Y. Moreno, Phys. Rev. Lett. **106**, 128701 (2011).
[35] L. M. Pecora and T. L. Carroll, Phys. Rev. Lett. **80**, 2109 (1998).
[36] I. Leyva, R. Sevilla-Escoboza, J. M. Buldú, I. Sendiña-Nadal, J. Gómez-Gardeñes, A. Arenas, Y. Moreno, S. Gómez, R. Jaimes-Reategui, and S. Boccaletti, Phys. Rev. Lett. **108**, 168702

(2012).
[37] T. K. D. M. Peron and F. A. Rodrigues, Phys. Rev. E **86**, 056108 (2012).
[38] B. C. Coutinho, A. V. Goltsev, S. N. Dorogovtsev, and J. F. F. Mendes, Phys. Rev. E **87**, 032106 (2013).
[39] W. Liu, Y. Wu, J. Xiao, and M. Zhan, Europhys. Lett. **101**, 38002 (2013).
[40] P. Ji, T. K. D. M. Peron, P. J. Menck, F. A. Rodrigues, and J. Kurths, Phys. Rev. Lett. **110**, 218701 (2013).
[41] X. Zhang, X. Hu, J. Kurths, and Z. Liu, Phys. Rev. E **88**, 010802(R) (2013).
[42] I. Leyva, A. Navas, I. Sendiña-Nadal, J. A. Almendral, J. M. Buldú, M. Zanin, D. Papo, and S. Boccaletti, Sci. Rep. **3**, 1281 (2013).
[43] X. Zhang, Y. Zou, S. Boccaletti, and Z. Liu, Sci. Rep. **4**, 5200 (2014).
[44] G. Su, Z. Ruan, S. Guan, and Z. Liu, Europhys. Lett. **103**, 48004 (2013).
[45] X. Hu, S. Boccaletti, W. Huang, X. Zhang, Z. Liu, S. Guan, and C. Lai, Sci. Rep. **4**, 7262 (2014).
[46] Y. Zou, T. Pereira, M. Small, Z. Liu, and J. Kurths, Phys. Rev. Lett. **112**, 114102 (2014).
[47] W. Zhou, L. Chen, H. Bi, X. Hu, Z. Liu, and S. Guan, Phys. Rev. E **92**, 012812 (2015).
[48] X. Zhang, S. Boccaletti, S. Guan, and Z. Liu, Phys. Rev. Lett. **114**, 038701 (2015).
[49] X. Zhang, Y. Zou, S. Boccaletti, and Z. Liu, Sci. Rep. **4**, 5200 (2014).
[50] E. A. Martens, M. J. Panaggio and D. M. Abrams, New Journal of Physics **18**, 022002 (2016).
[51] Y. Feng and H. Hong, Chinese Physics Letters **32**, 060502 (2015).
[52] S. Watanabe and S. H. Strogatz, Physica D **74**, 197 (1994).
[53] A. Pikovsky and M. Rosenblum, Phys. Rev. Lett. **101**, 264103 (2008).
[54] P. Mccullagh, The Annals of Statistics **24**, 787 (1996).